0273-2289/1559–0291 (Online)/07/136–140/859–874/$30.00

The Effects of Engineering Design on Heterogeneous Biocatalysis in Microchannels

Frank Jones,*[,1] Robert Bailey,[2] Stephanie Wilson,[1] and James Hiestand[1]

[1]University of Tennessee at Chattanooga, Chattanooga, TN 37403, E-mail: frank-jones@utc.edu; and [2]Loyola College in Maryland, Baltimore, MD 21210

Abstract

The results of a numerical study of the fundamental interactions of engineering design and micromixing on conversion in packed microchannels are presented. Previously, channel-based microreactors made of molded silicon plastic were designed, fabricated, and experimentally tested. These reactors have enzymes immobilized on the channel walls by various methods including layer-by-layer nano self-assembly techniques. They also contain molded packing features to add reactive surface area and to redistribute the fluid. An arbitrary but intuitively sensible packing arrangement was initially chosen and used in experimental studies. The current computer simulation study was undertaken to understand how static laminar mixing affects the conversion efficiency. The reactors previously used experimentally have been simulated using CFD-ACE+ multiphysics software (ESI CFD Inc., Huntsville, AL). It is found that packing significantly increases conversion when compared with empty channels over the entire flow rate range of the study ($0.25 < Re < 62.5$). The boost in conversion has an optimal point near $Re = 20$ for the particular geometry examined.

Index Entries: Catalase; enzyme; micromixing; microreactor; numerical simulation; heterogeneous catalysis.

Introduction

The field of miniaturizing chemical process devices has exploded in the last decade. This has led to extensive studies of the behavior in microscale fluidic channels. Most of these studies lie in the general categories of heat transfer *(1)*, mixing *(2)*, and chemical reaction *(3)*. Investigators are striving to acquire the ability to fully use the inherent advantages of the small scale. This work investigates heterogeneous catalysis in microchannels by numerical analysis. It follows up on previous experimental studies by the authors whereby enzymes were immobilized on polydimethylsiloxane (PDMS) microchannel walls by various techniques including layer-by-layer nano self-assembly *(4,5)*. The channels were created using molds fabricated by micro electro mechanical systems (MEMS) techniques. Reaction behavior in

*Author to whom all correspondence and reprint requests should be addressed.

these channels was physically studied and later simulated using CFD-ACE+ computational software *(6)*.

Static mixing is critical for homogeneous and heterogeneous chemical reaction in microchannels. Numerous physical and computational studies pursuing applications in DNA sequencing, chemical analysis, separation, and environmental monitoring have investigated micromixing in the last several years. Static mixing is accomplished on the microscale by excavating grooves or fabricating structures in the channels *(7–9)*. An attempt has even been made to optimize the number and pattern of the packing to achieve best mixing *(7)*. Mixing can also be accomplished by complex twisting, splitting, and rejoining pores in three dimensions *(3)*. Current microreactor research is to be applied to a broad array of applications including biofuels. Microreactors are being used to produce biodiesel fuel. Both mixing of the reactants and the transesterification reaction take place in microchannels reducing processing time from hours or days to minutes. Although each channel produces a very small quantity, banks of channels packaged in suitcase-sized devices can be used to produce enough fuel for individuals or small communities *(10)*.

It is the objective of this article to examine the effects of packing on mixing and heterogeneous conversion in microchannels. Also, the reactors are examined over a range of flow rates in order to find optimum operating conditions for a given design. The ultimate goal, beyond the present study, is to vary the packing feature size, shape, locations, and density in order to optimize the microchannel's ability to promote the reaction. As MEMS techniques and enzymes are very expensive, acquiring the ability to optimize the packing design will allow microreactors to become even smaller and perhaps more efficient. In the fabrication process, micromolds are made using 10-cm silicon wafers. Smaller reactors will allow more to fit on the same mold, making them significantly cheaper. Essentially, the microfluidics industry is following the path of the microelectronics industry in making smaller and smaller devices.

Theory

Descriptive Equations

The flow, mixing, and heterogeneous liquid–solid reaction in microchannels are described by a complex set of coupled nonlinear partial differential equations. For this study, several assumptions are introduced that simplify these equations significantly:

- The density and viscosity of the bulk mixture are determined by the primary constituent, water. The very small concentration of the substrate (hydrogen peroxide) has no appreciable effect on these parameters. This also leads to minimal heating from reaction owing to the high heat capacity of the water and the low level of

reaction per unit enzyme per unit flow, so the flow is considered to be isothermal.
- The flow is steady state, incompressible, and because of low fluid velocity and the smallness of the channels, laminar.
- Chemical reactions are heterogeneous, taking place only at solid–liquid interfaces wherein enzyme is present.

With these assumptions the flow field (velocity and pressure) within a reactor microchannel is determined by solving the following forms of the conservation of mass (continuity) and Navier–Stokes (momentum) equations:

$$\nabla \cdot \mathbf{V} = 0 \tag{1}$$

$$\rho \mathbf{V} \cdot \nabla \mathbf{V} = -\nabla p + \mu(\nabla^2 \mathbf{V}) + \rho \mathbf{g} \tag{2}$$

where **V** is Cartesian velocity vector (m/s), ρ is bulk mixture density (kg/m^3), p is pressure (Pa), μ is bulk mixture absolute viscosity (N·s/m^2), and **g** is gravitational acceleration vector (m/s^2). The steady-state concentration field is governed by:

$$\mathbf{V} \cdot \nabla C_i - D_i \cdot \nabla^2 C_i = 0 \tag{3}$$

where, i is species indicator (one equation for each species), C_i is concentration of species i (M), and D_i is diffusivity of species i in solvent (m^2/s). The kinetics of the heterogeneous chemical reaction that takes place at the solid–liquid interfaces is described using the Michaelis–Menten model:

$$v = \frac{V_{max}[S]}{k_m + [S]} \tag{4}$$

where v is reaction rate (mol/[s·m^2]), [S] is substrate concentration at the solid surface (M), V_{max} is the maximum reaction rate (mol/[s·m^2]) $V_{max} = k_{cat}$ [E], k_m is Michaelis constant (concentration that gives $v = V_{max}/2$) (M), k_{cat} is turnover number (s^{-1}), and [E] is enzyme concentration at the solid surface (mol/m^2).

Boundary Conditions

The boundary conditions associated with flow and reaction within microchannels are as follows. At the channel inlet, a uniform velocity distribution and substrate concentration were specified whereas at the channel exit, a fixed pressure boundary condition was assigned. A no-slip boundary condition (**V** = 0) was applied at all solid surfaces. If no enzyme is present on a solid surface, the concentration boundary condition is given by:

$$D_s \times \frac{d[S]}{dn} = 0 \tag{5}$$

where D_s is the diffusivity of substrate in the solvent (m^2/s) and n is distance in direction normal to the solid surface (m). If enzyme is present at the surface, the following boundary condition, which includes Michaelis–Menten kinetics, was applied to implement the steady, heterogeneous catalysis reaction:

$$-D_s \times \frac{d[S]}{dn} = \frac{V_{max} \times [S]}{k_m + [S]} \quad (6)$$

Dimensionless Parameters

Two dimensionless parameters are of particular interest in this study. The first is the mass transfer Peclet number (*Pe*), which represents the ratio of advection to diffusion mass transfer rates. This parameter is defined as:

$$Pe = \frac{Ud}{D_s} \quad (7)$$

where U is velocity magnitude (m/s) and d is the smallest channel cross dimension (m). The second dimensionless parameter is the Reynolds number (*Re*), given by:

$$Re = \frac{\rho U d}{\mu} \quad (8)$$

The Reynolds number represents the ratio of inertial forces to viscous forces within the moving fluid, and it is a determining factor in transition from laminar to turbulent flow. As already mentioned, all flows in this study were laminar.

Numerical Solution Method

The differential equations were solved numerically using the CFD-ACE+ computational package developed by ESI CFD Inc., located in Huntsville, Alabama *(11)*. CFD-ACE+ is a finite volume-based code that uses a variation of the semiimplicit method for pressure-linked equations consistent (SIMPLEC) algorithm *(12)*. As with all finite volume methods, two major approximations are used:

- The physical domain is broken down into a series of small control volumes (cells). The resultant collection of cells is referred to as the computational grid.
- The governing differential equations are replaced by a set of algebraic finite difference equations that approximate the requirements of the differential equations on each cell.

In general, the velocity, pressure, and concentration fields are linked, but owing to the small substrate concentrations considered in this study, the concentration field could be decoupled to enhance computational efficiency. The solution algorithm proceeds in two major steps. First, the velocities and pressures at the cell centers are calculated using an iterative pressure-correction approach (SIMPLEC). Once these flow field variables are determined, they are introduced into the approximated species conservation equation, and the concentrations at the cell centers are calculated iteratively *(11)*. CFD-ACE+ has been applied previously by the authors to simulate flow and reaction within microchannels, and validation through comparison with experimental data is described in ref. *6*.

Modeling and Simulation Procedures

Two separate three-dimensional representations (models) of a single microreactor channel were created using CFD-ACE+. In each case, the channel was 500 μm wide (*x*-direction) by 125 μm deep (*y*-direction) by 50,000 μm long (*z*-direction). The first model, which considered a channel without internal features, used a structured grid with approx 720,000 cells. Grid points were clustered near the channel walls to more accurately resolve concentration gradients there. A portion of the grid is shown in Fig. 1A. A second model was developed for a channel with internal features that were shaped like triangular prisms. Because of the more complex geometry, an unstructured grid consisting of just over 1,000,000 cells was used. A portion of this grid is presented in Fig. 1B. Sensitivity studies performed with other grids indicated that the two earlier models provided sufficient resolution to capture important trends in the solutions. The chemical reaction considered in all of the simulations was the breakdown of hydrogen peroxide (H_2O_2) into oxygen and water in the presence of catalase (the enzyme catalyst):

$$H_2O_2 \xrightarrow{\text{Catalase}} H_2O + \frac{1}{2}O_2 \tag{9}$$

An active catalase surface concentration of 1.0×10^{11} molecules/cm^2 was assigned at all solid surfaces wherein enzyme was present, and the H_2O_2 concentration at the channel inlet was set to 0.0147 *M* (500 ppm). The fluid flow, mass transfer, and reaction kinetics parameters were taken from the open literature and are shown in Table 1. All computations were performed on personal computers equipped with a 3.0 or 3.6 GHz Intel Pentium 4 processors and 2 GB of random access memory (RAM). The computational times ranged between 7 and 11 h depending on Reynolds number and the presence or absence of internal features.

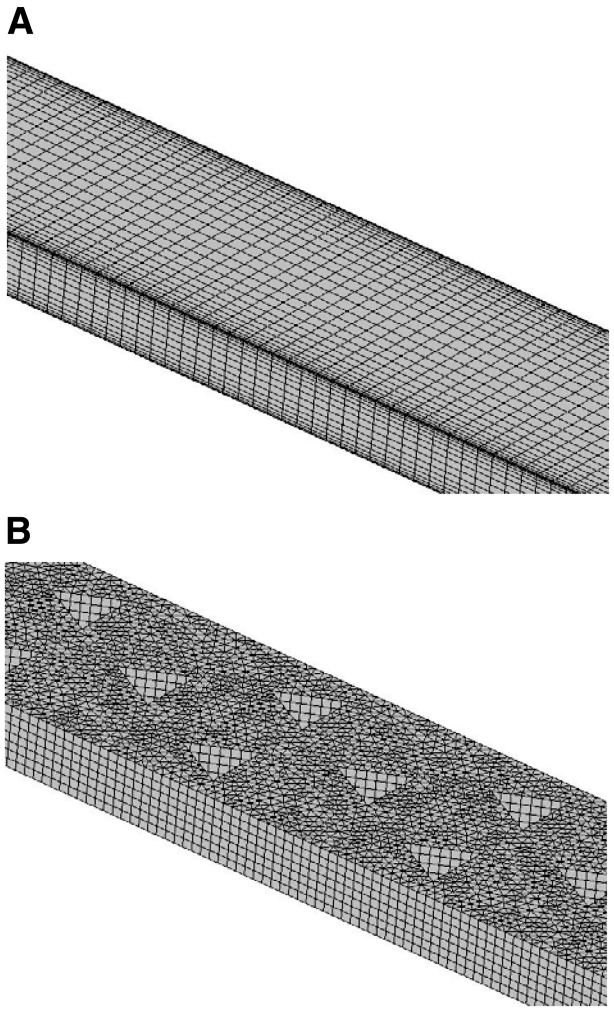

Fig. 1. (A) A portion of the structured grid used for a microreactor channel with no internal features. **(B)** A portion of the unstructured grid used for a microreactor channel with internal features.

Table 1
Flow, Mass Transfer, and Kinetics Parameters

Property	Symbol	Value
Bulk mixture density *(13)*	ρ	998 kg/m^3
Bulk mixture kinematic viscosity *(13)*	υ	1.31×10^{-6} m^2/s
Diffusivity of H_2O_2 in water (25°C)	D_s	1.0×10^{-9} m^2/s
Michaelis constant for breakdown of H_2O_2 catalyzed by catalase *(14)*	k_m	0.025 *M*
Turnover number for breakdown of H_2O_2 catalyzed by catalase *(14)*	k_{cat}	1.0×10^7 s^{-1}

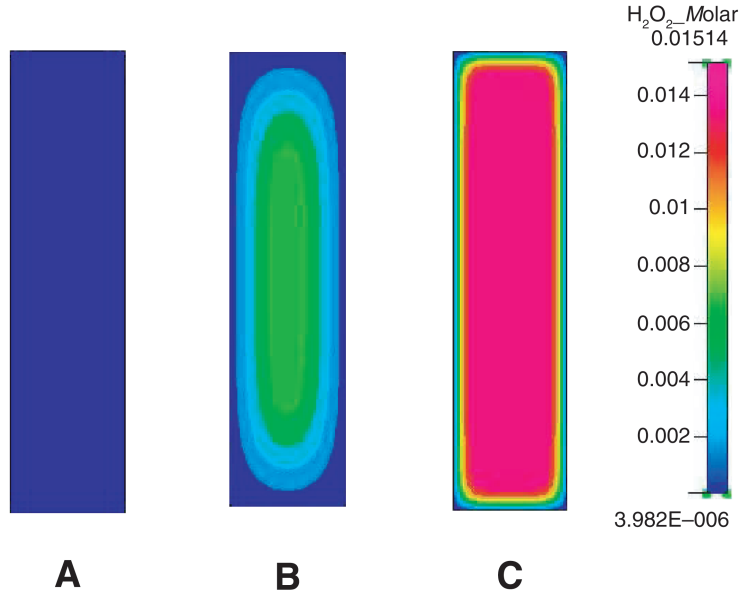

Fig. 2. Concentration profiles of the exit planes of various reactor channels. **(A)** Cross-section 50 × 12.5 μm², **(B)** 500 × 125 μm², and **(C)** 5000 × 1250 μm².

Table 2
Reactor Performances for Various Channel Sizes

Scale (μm) (length × width)	Flow rate (mm^3/s)	*Re*	*Pe*	*X* (%)	Δ*P* (Pa)
5000 × 1250	166.7	25	33,375	3.5	25
500 × 125	16.67	2.5	3338	62.5	1500
50 × 12.5	0.167	0.25	334	100	156,000

Results and Discussion

The Effect of Scale on Conversion in Microchannels

The effect of decreasing reactor cross-section on conversion should be dramatic for heterogeneous catalysis in channels simply because of increased proximity of reactant molecules to enzyme-coated walls as the scale becomes smaller. Previous experimental studies *(4,15)* used 50 mm long channels with 500 μm by 125 μm cross-sections with 1% (by mass) surface coverage of immobilized enzyme. The level of conversion in channels an order of magnitude larger (5000 × 1250 μm²) and an order of magnitude smaller (50 × 12.5 μm²) are compared with the experimental (nominal) scale. Each scale has a flow rate and surface area 100 times smaller than the next for proper comparison. The feed to all channels is 500 ppm hydrogen peroxide in water.

The calculated conversions at the exits for the three sizes are shown as concentration profiles in Fig. 2 and numerically in Table 2. The largest

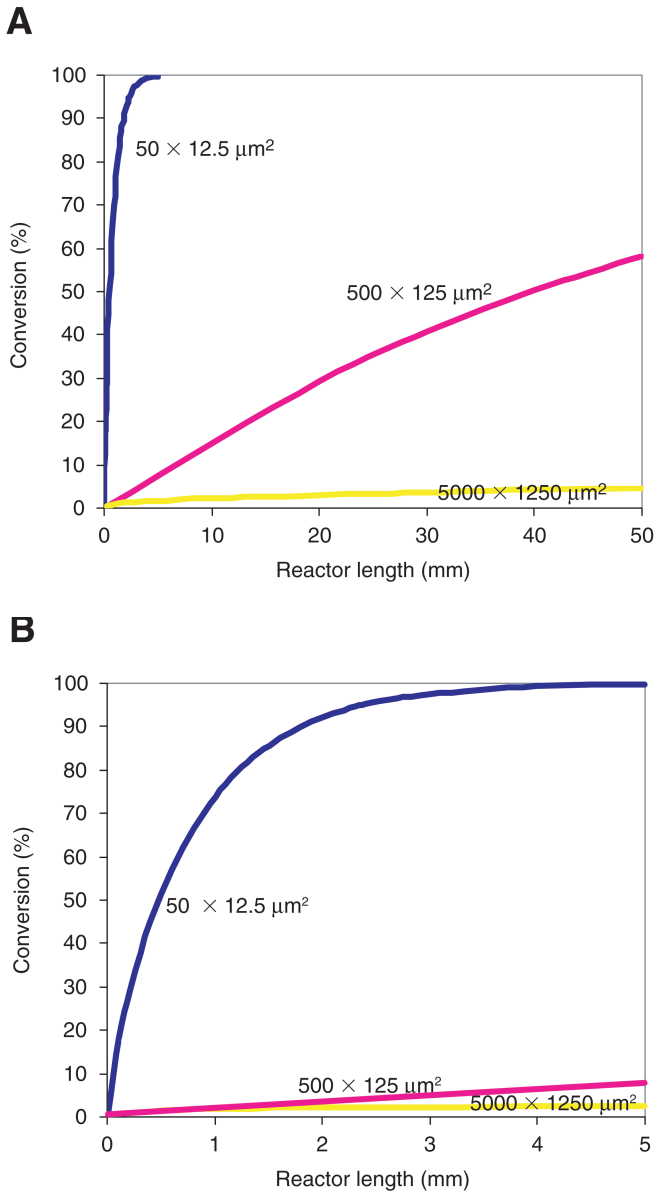

Fig. 3. (A) Conversions along the lengths of the reactor channels of Fig. 1. **(B)** Detail of the conversion profiles of the first 5 mm of the channels in Fig. 3 **(A)**.

channel has a conversion of 3.5%; the experimental scale, 62.5%; and the smallest channel, virtually 100% at their exits (50 mm length). In fact, the smallest channel reached complete conversion far before the exit. Fig. 3A shows the conversion vs length behavior in the channels. The channel with the smallest cross-section reaches 99% conversion in less than 5 mm. Part B of Fig. 3 is a blowup of the first 5 mm of the reactor channels. At the 3 mm point, the smallest scale has about 98% conversion compared

with 4% for the nominal scale, which is an increase of 2350% in the number of reactions per unit enzyme per unit flow.

The pressure drops grow dramatically as cross-section decreases (from 25 to 156,000 Pa). Although a pressure drop of 156,000 Pa is not experimentally prohibitive *(4)*, Fig. 3A reveals that a proper design for the smallest scale would be a reactor only 5 mm in length. The resulting pressure drop of about 1560 Pa would be almost identical to the full length nominal reactor. Clearly, smaller reactors would be cheaper to fabricate by standard MEMS techniques because more reactors would fit on a standard 10 cm wafer. Also, the smaller molded reactor would be cheaper to coat with (very expensive) enzyme *(5)*. Reynolds numbers are also shown in Table 2. They vary owing to the characteristic length (the smallest cross dimension) changing by a factor of 10 for each scale, but all flows are laminar.

Only lateral diffusion to flow can carry a reactant molecule to a wall for reaction in an empty channel. Parts (B) and (C) of Fig. 2 clearly show that centrally located process fluid remains largely unreacted at the channel exits. The Peclet number is a measure of the ratio of advection (transport owing to bulk fluid motion) to diffusion mass transfer. Lower Peclet numbers allow for adequate lateral diffusion in the 50 mm channel length and lead to higher conversions. As shown in Table 2, for Peclet number significantly higher than 334, advection dominates diffusion and fluid redistribution is required to improve conversion.

The Effect of Static Mixing on Conversion: Packed Channels

Packing features are added to the empty channels to improve conversion by providing fluid redistribution and adding reactive surface area with coated packing. Fluid redistribution refers to the break-up of flow patterns to enhance fluid-solid contact. Because the flow is laminar, this is not mixing in the traditional sense. The term chaotic advection is sometimes used to describe this laminar phenomenon. Figure 4 shows a detail of the velocity field in a channel with the packing feature pattern used in all packed simulations and a flow rate of 25 cc/min ($Re = 62.5$). Triangular packing features with a perimeter of $125 \times 125 \times 140$ μm^3 and the full channel depth of 125 μm are located in a repeating pattern of three per 500 μm length (referred to as a unit cell) for a total of 300 features in the 50 mm channel. The packing adds 17.2% surface area and subtracts 10.5% channel volume. Therefore, packing reduces process fluid residence time by 10.5% when compared with equal flow rate simulations in empty channels.

Conversions for a Reynolds number range of 0.25 to 62.5 are shown in Fig. 5 for channels with and without packing features. Also shown are conversions for channels with uncoated packing, which will be discussed later. There are large improvements in conversion at all flow rates owing to packing except at $Re = 0.25$ wherein all channels achieve virtually 100% conversion. This is in spite of the fact that there is 10.5% less residence time for reaction in packed channels.

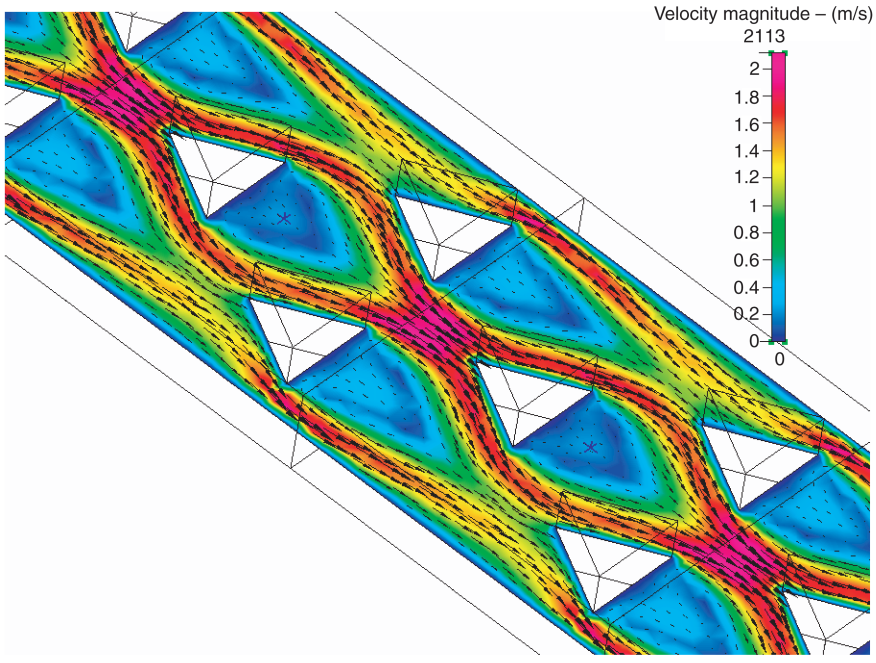

Fig. 4. Detail of the velocity field for *Re* = 62.5 in packed channel with a 500 × 125 μm^2 cross-section. Packing is in a repeating pattern for the entire 50 mm long channel.

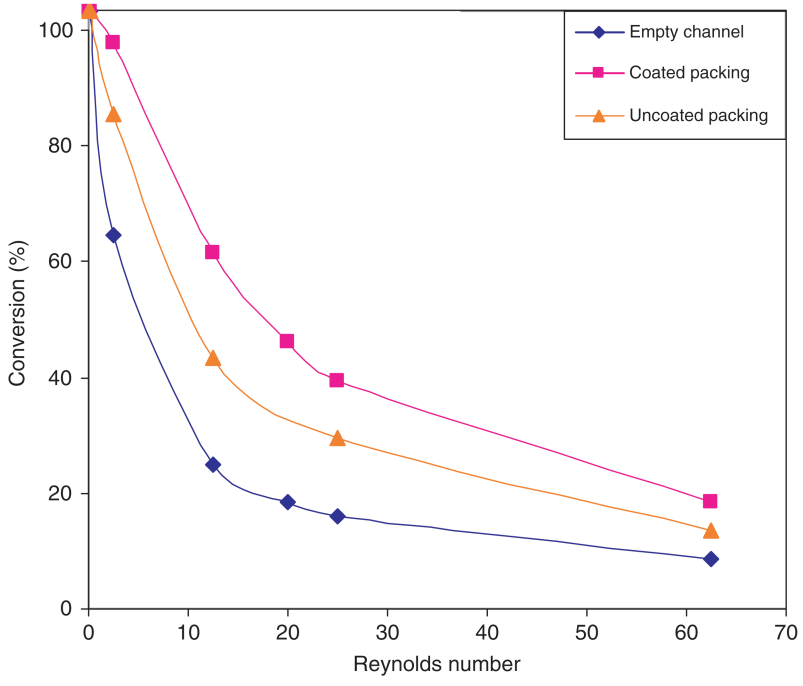

Fig. 5. Conversions for channels with and without packing and with uncoated packing at various Reynolds numbers.

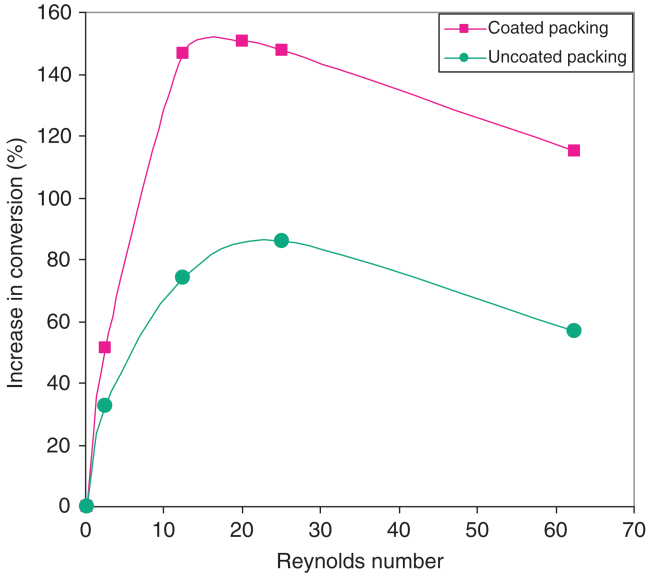

Fig. 6. Percentage increase in conversion owing to packing.

The level of conversion improvement varies greatly over the range of flow rates. For example, at a flow rate of 1 cc/min (Re = 2.5), conversion increases from 62.5% for an empty channel to 94.5% for a packed channel. The conversion improvements over the entire range of flow rates for coated and uncoated packing are shown in Fig. 6. A peak in increase in conversion for coated packing over empty channels occurs near Re = 20. Here, the packed channel has 151% more conversion than an empty one.

This discovery suggests an optimal use of this design. Previous experimental work was performed using packed channels and a nominal flow rate of 1 cc/min (Re = 2.5). Simulations show that the maximum beneficial effect of packing on conversion is at 8 cc/min, which is eight times the nominal flow rate but still has almost half the conversion (44.7% vs 94.5%). This yields a 278% increase in reactions per enzyme. This increase in enzyme effectiveness can be explained by increased chaotic advection as flow speeds up. In fact, the number of reactions performed by each enzyme in packed channels increases over the entire flow rate range, because conversion never decreases as much as residence time. This behavior is consistent with experimental results in similar reactors wherein urea was reduced using immobilized urease *(5)*. Table 3 contains conversions, Peclet numbers, and pressure drops for empty and packed channels at various flow rates. Packing increases pressure drop significantly. At a flow rate of 1 cc/min, an empty channel has a pressure drop of 1500 Pa, whereas packing causes an increase to 4100 Pa, a factor of about 2.73. This factor increases with flow rate, such that at a flow rate of 25 cc/min, the factor is 5.76. Pressure drops for packed channels also increase significantly more than linearly as flow rate increases.

Table 3
Conversions and Pressure Drops for Empty and Packed Channels

Re	Flow rate (cc/min)	*Pe*	ΔP (Pa) (empty)	*X* (%) (empty)	ΔP (Pa) (packed)	*X* (%) (packed)
0.25	0.1	334	200	100	400	100
2.5	1.0	3338	1500	62.5	4100	94.5
12.5	5.0	16,688	7900	24.2	24,600	59.6
20	8.0	26,700	12,700	17.8	44,900	44.7
25	10	33,375	15,800	15.4	60,500	38.2
62.5	25	83,438	39,800	8.4	229,300	18.0

Figure 7 shows the velocity fields taken at the vertical midplane in the channel entry regions for each of four flow rates. Four repeating unit cells (a total length of 2 mm of the 50 mm channel) are shown for each case. Entry lengths for hydrodynamically fully developed flows have been estimated from these figures in multiples of 0.5 mm. Entry lengths are 1, 1.5, 2, and 2.5 mm for Reynolds numbers of 0.25, 2.5, 25, and 62.5, respectively.

Three distinct flow fields appear in packed channels over the entire Reynolds number range of this study. The two slower flow rates ($Re = 0.25$, 2.5) appear to have creeping flow around packing features and slow flow near the outside walls that mostly returns to and mixes with more centrally located fluid (Fig. 7, top 2 images). Faster flow at $Re = 25$, has fast flow along the two upstream walls of each triangle and significant dead spots behind each triangle. There is also significant channeling around the central triangles. At the fastest flow rate ($Re = 62.5$), separate channels develop between the outside walls and their neighboring triangles (Fig. 7, bottom image). These channels remain largely separate from the central flow creating a significant opportunity for a large amount of fluid to flow near a reactive surface that is not seen in slower flow rates.

The Effect of Static Mixing in Packed Channels: Uncoated Packing

Packing adds reactive surface area and static mixing to increase conversion. In order to separate these two effects, simulations were performed with the same packing configuration but with the surfaces of the triangles that are exposed to the flow not coated with enzyme. Uncoated packing reduces both reactor volume and residence time by 10.5% and reduces the active reaction area by 8.4% when compared with empty channels. In spite of these handicaps, reactors with uncoated packing perform significantly better than empty channels at all but the slowest flow rate ($Re = 0.25$ is virtual creeping flow) as shown in Fig. 5. For example, at $Re = 25$, fluid redistribution using uncoated triangles increases conversion from 15.4% to 28.6%. Coating the packing

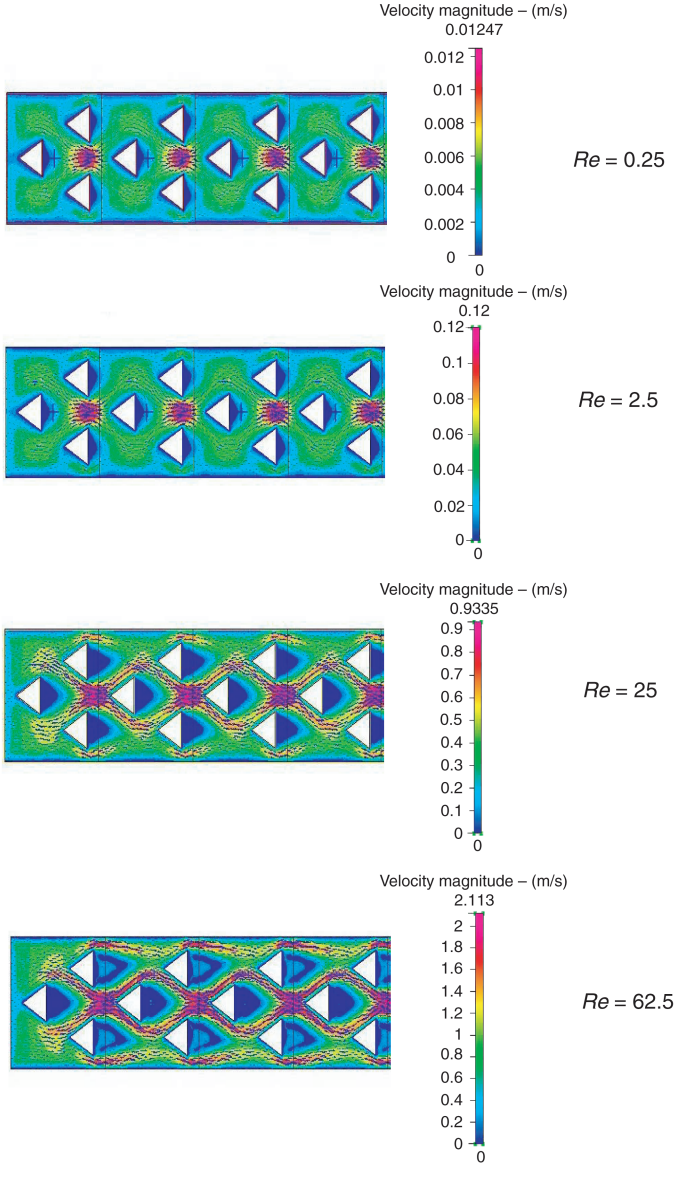

Fig. 7. Top view of the velocity fields in the vertical midplane near the channel inlet for various Reynolds number. Velocity scales at right.

increases the reactive surface area by 27% (vs uncoated) and further increases conversion to 38.2%. Figure 6 shows that the effect of static mixing on conversion over empty channels varies with Reynolds number and peaks around $Re = 20$, as it did for coated features.

The Effect of Flow Direction Using Triangular Packing

When the flow direction in a packed channel is reversed, a significantly different flow field results. Figure 8 shows flow into the flat base of

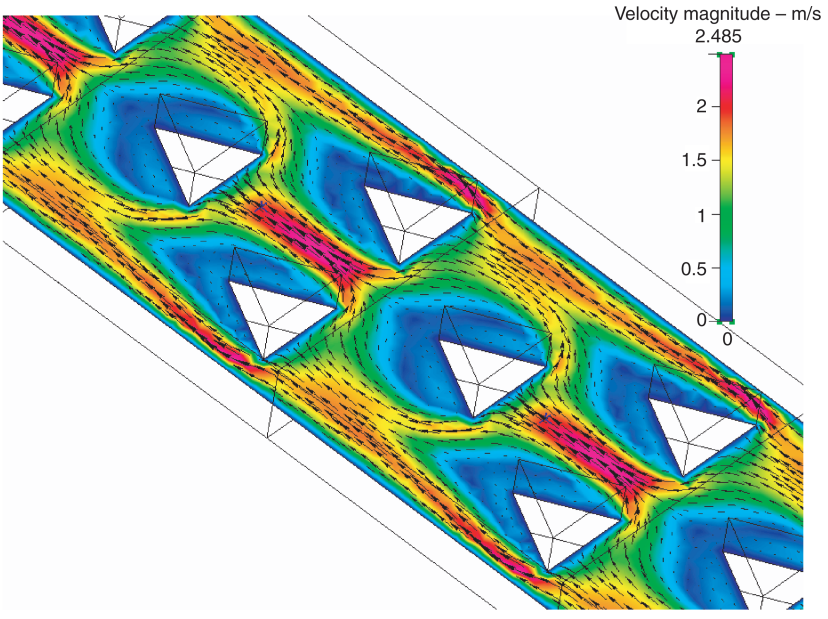

Fig. 8. Velocity field for reverse process flow at *Re* = 62.5.

the triangles for a Reynolds number of 62.5. As the packing now directs some flow in a direction lateral to the bulk flow, static mixing should be increased when compared with flow into the triangle points *(2)*. It follows that increased mixing should increase conversion. However, inspection of the flow shows slow flow on both downstream faces of the triangles, reducing presentation of reactive surface area to the faster flows, which are essentially the majority of the process fluid, and hence, dictate the level of conversion. Ultimately, conversions for the reversed flow are found to be about the same as for flow into the points of the triangles. Flow into the flats increased conversion in all cases, but always by less than 1%. Simulations using uncoated packing with flow into the flats also resulted in conversions virtually the same as those with flow into the points.

Conclusions

Heterogeneous catalysis in microchannels has been successfully simulated over a broad range of flow rates. It is found that static mixing (laminar flow redistribution) using triangular packing features significantly increases conversion over the entire range of flow rates ($0.25 < Re < 62.5$) when compared with the conversions in empty channels. There is a peak improvement to conversion at a Reynolds number near 20 for both coated and uncoated packing. Changing the mixing patterns significantly by reversing the flow into the bases of the triangles does not improve conversions.

Acknowledgments

The authors gratefully acknowledge the support of the State of Tennessee through a Center of Excellence in Applied Computational Science and Engineering Grant (R04-1302-007).

References

1. Ameel, T. A. (1997), *Int. Comm. Heat Mass Transfer* **24,** 1113–1120.
2. Nguyen, N. T. and Wu, Z. (2005), *J. Micromech. Microeng.* **15,** 1–16.
3. Zheng, A. I., Jones, F., Fang, J., and Cui, T. (2000), in *Proceedings of the Fourth International Conference on Microreaction Technology* (IMRET IV), pp. 284–292.
4. Jones, F., Forrest, S., Palmer, J., Lu, Z., Elmore, J., and Elmore, B. (2004), *Appl. Biochem. Biotechnol.* **113–116,** 261–272.
5. Wen, J., Elmore, B., and Jones, F. (2007), submitted to *Biotechnol Bioeng*.
6. Bailey, R., Jones, F., Fisher, B., and Elmore, B. (2005), *Appl. Biochem. Biotechnol.* **121–124,** 639–652.
7. Wang, H., Iovenitti, P., Harvey, E., and Masood, S. (2002), *Smart Mater. Struct.* **11,** 662–667.
8. Lin, Y., Gerfen, G. J., Rousseau, D. L., and Yeh, S. R. (2003), *Anal. Chem.* **75,** 5381–5386.
9. Wang, H., Iovenitti, P., Harvey, E., and Masood, S. (2003), *J. Micromech. Microeng.* **13,** 801–808.
10. Jovanovich, G. (2006), *Ind. Bioprocessing* **28(4),** 6.
11. ESI CDF Inc (2006), *CFD-ACE+ V2006 User Manual,* Huntsville, AL.
12. Van Doormaal, J. and Raithby, G. (1984), *Numer. Heat Transfer* **7,** 147–163.
13. Crowe, C., Roberson, J., and Elger, D. (2001), *Engineering Fluid Mechanics*, 7th ed. John Wiley & Sons Inc., New York.
14. DeTurck, D., Gladney, L., and Pietrovito, A. (1996), *The Interactive Textbook of PFP 96*, http://dept.physics.upenn.edu/courses/gladney/mathphys/subsection4_1_7.html, University of Pennsylvania, Philadelphia, PA.
15. Jones, F., Lu, Z., and Elmore, B. (2002), *Appl. Biochem. Biotechnol.* **98–100,** 627–640.